SIMULATIONS OF TRANSVERSE HIGHER ORDER DEFLECTING MODES IN THE MAIN LINACS OF ILC

C.J. Glasman[†‡], R.M. Jones[†‡], I. Shinton[†‡], G. Burt[§‡,]
[†]The University of Manchester, Manchester M13 9PL, UK
[‡]Cockcroft Institute of Science and Technology, Daresbury, Cheshire WA4 4AD, UK
[§]Lancaster University, Lancashire, LA1 4YR, UK

Abstract

We investigate the electromagnetic field excited by a train of multiple bunches in the main superconducting linacs of the International Linear Collider (ILC). These e.m. fields are represented as a wake-field. Detailed simulations are made for modes constituting the long-range wake-field in new high gradient cavities. In particular, we focus our study on the transverse deflecting modes in high gradient cavity designs known as "Ichiro", in which the central cells have iris radius of 30 mm. These cavities have a reduced iris compare to the TESLA design and will have more intense wake-fields. Several software packages solving the electromagnetic field, employing different algorithms have been used to model the cavity. The performance of these codes is compared.

INTRODUCTION

The ILC is an electron-positron collider and will employ superconducting radio frequency (SRF) cavities in its main linacs to accelerate the charged bunches to a centre of mass energy of 500GeV at collision (in the first phase and to 1 Tev in the upgrade scenario). Meeting its design luminosity of $2x10^{34}$ $cm^{-2}s^{-1}$ [1] places strong demands on the performance of many systems and on the the linacs in particular, where the transverse wake-field can lead to emittance growth in the beam and a consequent luminosity reduction. In the worst case this can lead to a beam break up mode being developed along the bunch train if the wake-field is not adequately damped..

The ILC baseline technology for the main linac SRF cavities is the TESLA [2] technology and aims at peak accelerating gradients of 35 MV/m. The injected beam must be accelerated from 15 GeV to 250 GeV down one arm of the linac, passing through more than 7000 cavities. The cavities are grouped in cryomodules containing 8 or 9 cavities. To date, of the order of ten cryomodules have been produced with a gradient that meets the design requirements. Clearly, the reproducible of cavity performance in industrial fabrication with the necessary yield is a significant challenge for the ILC design phase.

Intense international research is ongoing into optimal cavity designs, with the current goal to achieve gradients in excess of 50MV/m. These high gradient cavities will allow a smaller footprint for the collider and represent a significant initial cost saving. Furthermore, the cavities would form a major part of the proposed upgrade to 1TeV.

Two main alternative designs are incorporated into the ILC Reference Design Report [2], a re-entrant shape with development based at Cornell University and a design at KEK based on a low-loss cavity shape known as the "Ichiro" cavity. The latter is illustrated in Fig 1. In both designs the magnetic field on the niobium surface has been reduced by carefully reshaping the cells. The present superconducting materials impose a 180 mT maximum field that can sustained on the surface before superconductivity breaks down. Thus there is a potential for better performance than that of the baseline TESLA.

Improvement has been demonstrated in single cell tests of both designs in which gradients in excess of 51MV/m have been achieved [3]. Full 9-cell cavities are being constructed and tested though.

Figure 1: Ichiro Cavity fabricated at KEK

Here we focus on a symmetric Ichiro design which has irises of 30 mm in radius and 40 mm beam pipes attached at either end of the cavity (with a cut-off frequency 2.196 GHz). This design incorporates reduced iris dimension and reshaped cells, compared to the TESLA which has 35 mm irises and accordingly it is expected to have repartitioned higher order modes (HOM) Thus the long range wake-field will differ from that in the TESLA cavities both in the maximum of the envelope of the field and in the distribution. We do not analyse the influence of the coupler dampers in this paper. However, we do provide a simulation of the wake-field and it's modal components. In particular, we investigate trapped modes which are not be damped by the couplers. The first dipole mode field for example, illustrated in Fig 2, is located in the vicinity of the coupler and is readily damped. However, the field for a number of higher modes are trapped and these are discussed in the next section. These modes can only be damped in the end cells where the couplers are located, by modifying the geometry of the

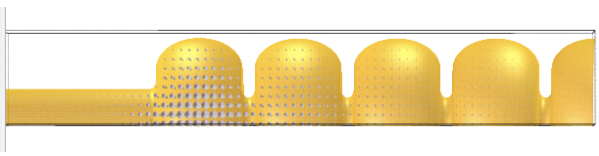

Figure 2: Ichiro cavity geometry modelled in GdfidL and showing first dipole mode field.

cells in order to re-allocate the mode distribution. The design of these couplers relies heavily on an accurate

simulation of the cavity structure using electromagnetic field computer codes.

We provide a comparison of the dipole mode properties calculated by several widely used software packages which model the cavities in either two or three dimensions. These codes use either the finite element or finite difference algorithms in order to model the geometry with a characteristic mesh.

CAVITY EIGENMODES

To characterise the cavity we used the eigensolver components in the following packages: GdfidL, MAFIA2D, HFSS, and Analyst. The first two rely on finite difference algorithms in order to solve for the fields and frequencies and the latter two use finite element-based algorithms. HFSS and GdfidL use a 3D meshing algorithm whereas we used the 2D components of MAFIA2D and Analyst. In performing the simulations dipole modes were selected by enforcing symmetry planes for 3D solver simulations. In all cases we assigned magnetic-wall boundary conditions on the ends of the beam pipes and, initially, these pipes had lengths equivalent to 1.5 cells.

MAFIA and HFSS were run on single desktop machines, while we employed linux clusters to run parallel versions of GdfidL and Analyst under PVM and MPI respectively.

We discretised the cavity using 0.8 mm spaced cells with the finite difference code GdfidL, creating a mesh with more than 16×10^6 cells and using in excess of 13 GB of memory, for half the cavity. By performing two simulations, firstly with a magnetic boundary and lastly with an electric boundary, the modes in a complete nine-cell geometry could be recreated for the 4.5 cavity plus beam tube simulated. The eigenmodes were extracted up to 4 GHz and the phase for each mode calculated using the Floquet field relation [4]. The Brillouin diagram in Fig. 3 shows the discrete eigenmodes and the continuous band structure. The latter bands were obtained from inner cells of the cavity subjected to infinite periodic boundary conditions.

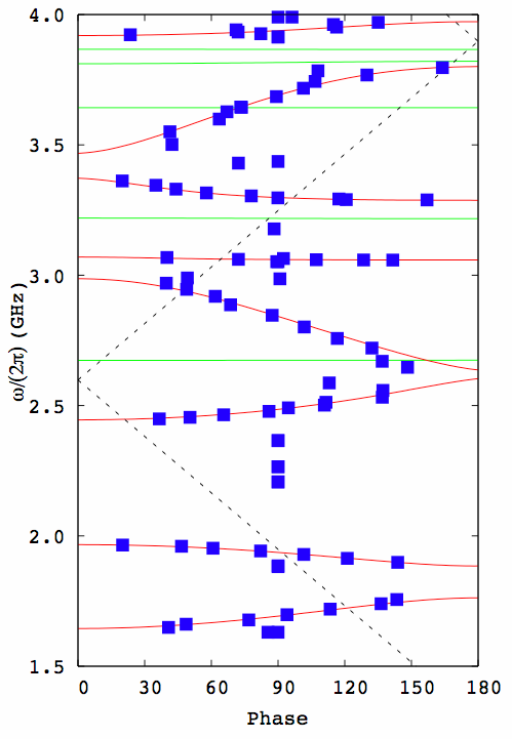

Figure 3: Dispersion curves showing dipole (red) and sextupole (green) bands, with cavity modes (blue).

The discrete modes are required to lie on the periodic curves. However, those corresponding to beam pipe modes and above the cut-off frequency are noticeably separated from the curves. Modes which are strongly influenced by the end cell geometry are also somewhat displaced and are very sensitive to the dimensions of the end cells.

In the simulations with the finite difference code MAFIA, we discretised the 2D system into 500,000 cells and sought dipole modes frequencies lower than 4 GHz. The loss factors versus mode frequencies are displayed in Fig. 4 for both the MAFIA and GdfidL simulations.

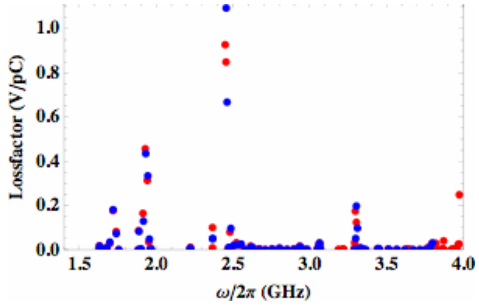

Figure 4: Loss factors calculated using GdfidL (red) and MAFIA (blue).

We also used the eigenmode solver of the 3D computer code HFSS 8.5 with an adaptively refined mesh of linear finite elements. Refinement ceased once a tolerance of better than 0.005% in the frequency was achieved, on a final mesh of approximately 550,000 elements. The dipole modes in the lower three bands were calculated in three separate runs, with a new refinement in each case.

Second order finite elements were used in Analyst to model the cavity in two dimensions. The mesh was adaptively refined for the first three bands until a specified convergence was reached. The results obtained with the code Analyst are for meshes containing more than 10^6 elements and with a mean element spacing less than 0.5mm. These simulations were rapidly performed using a linux cluster in parallel and a method of full decomposition of the finite element matrix.

Comparison of results

The modal frequencies and R/Qs are presented in Tables 1 and 2 for the first three bands. Before making a detailed comparison of the data presented in the table it is worth pointing out that the accuracy of the calculation is expected to decrease as the frequency increases as the

wavelength becomes comparable to the mesh size. This general statement is readily verified in glancing through the data in which the higher the frequency, the larger the discrepancy between the four codes presented. For example, in the first band, presented in Table 1, the differences between the calculated frequencies are less than 1 MHz. Similarly, in the second band the Analyst and GdfidL are separated by less than 1 MHz, while HFSS differs at most by 1.7 MHz. MAFIA results are the furthest displaced with a uniform 3 MHz difference.

The behaviour in the third band is markedly different. GdfidL and MAFIA results differ by up to 7 MHz. HFSS shows similar, though smaller, frequency deviation from GdfidL. The Analyst results, which were performed with the highest resolution mesh, show unexpected behaviour. For the lower four modes within the third dipole band, where there is low group velocity, the frequencies are 1 MHz shifted from GdfidL. However, this begins to rise from the fifth mode and the final mode in the band is shifted by 26 MHz.

Shifts greater than 10 MHz would normally be associated with significant changes in the geometry (to contrast, a shift of 8 MHz occurs for a 1 mm change in the cell radius at the equator due to electron-beam welding [5]). To investigate this effect further GdfidL simulations were performed in which the end-cell geometry was perturbed by 0.05 mm in the horizontal half axis of the equator ellipse.

For this end-cell perturbation certain modes show significant sensitivity in particular the lowest two dipole modes in the first band shift by ~0.1 MHz. The separation between these modes differed significantly according to which codes were used and this is understood to be due to the low group velocity of the modes in this region. The difference for the lowest third band mode at 2.4488 GHz was just 0.005 MHz compared to the 0.2 MHz shift observed for the higher modes in the band. Fig. 5 shows the electric field in the mode at 2.4488 GHz, which is trapped in the inner cells of the cavity.

To contrast this trapped mode, in Fig. 6 a mode which exists throughout the cavity and through to the region of the beam tubes is illustrated. This latter mode is located in the third band and it is a 'multi-cavity' mode. These types of modes will exhibit a sensitivity to the length of the beam tubes, and as the simulations with

Table 1: Modal frequencies, $\omega/2\pi$ (GHz) and R/Qs (Ohms/cm/cm) for the first two dipole bands, calculated using GdfidL, MAFIA, HFSS and Analyst

GdfidL short $\omega/2\pi$	GdfidL R/Q short	GdfidL long $\omega/2\pi$	GdfidL long R/Q	MAFIA short $\omega/2\pi$	MAFIA R/Qs	HFSS short $\omega/2\pi$	Analyst short $\omega/2\pi$	Analyst short R/Q
1.63035	0.385	1.63035	0.379	1.63094	0.342	1.63032	1.62941	
1.63044	0.050	1.63045	0.086	1.63109	0.119	1.63062	1.62950	
1.64907	0.039	1.64907	0.038	1.64927	0.045	1.64888	1.64816	
1.66102	0.080	1.66102	0.070	1.66133	0.066	1.66097	1.66015	
1.67769	0.202	1.67769	0.171	1.67812	0.150	1.67772	1.67687	
1.69757	0.568	1.69757	0.690	1.69813	0.713	1.69777	1.69679	
1.71897	3.639	1.71897	3.759	1.71971	3.713	1.71923	1.71826	
1.73962	1.672	1.73962	1.529	1.74050	1.473	1.73994	1.73892	
1.75578	0.002	1.75578	0.000	1.75680	0.000	1.75613	1.75511	
1.88201	0.000	1.88201	0.001	1.88507	0.000	1.88367	1.88158	
1.88522	1.615	1.88523	1.533	1.88830	1.541	1.88678	1.88480	
1.89865	0.004	1.89865	0.044	1.90172	0.073	1.90004	1.89815	
1.91403	3.041	1.91403	2.581	1.91709	2.380	1.91529	1.91343	
1.92902	8.365	1.92902	8.283	1.93207	7.950	1.93007	1.92832	
1.94216	5.705	1.94216	5.909	1.94519	6.079	1.94296	1.94135	
1.95274	0.623	1.95274	0.801	1.95576	0.867	1.95348	1.95183	
1.96044	0.082	1.96044	0.057	1.96343	0.040	1.96105	1.95943	
1.96509	0.052	1.96509	0.047	1.96807	0.039	1.96564	1.96402	
2.22302	0.174	2.20725	0.001	2.22185	0.083			
2.22302	0.004	2.20725	0.032	2.22185	0.083			
		2.26551	0.099	2.36820	0.746		2.39381	1.097
		2.26551	0.228	2.36822	0.745		2.39381	1.108
2.36660	0.128	2.36541	0.037	2.36822	15.739		2.39381	14.884
2.36660	1.499	2.36541	0.985	2.36822	9.588		2.39381	9.700

Table 2: Modal frequencies, ω/2π (GHz) and R/Qs (Ohms/cm/cm) for the 3rd dipole band, calculated using GdfidL, MAFIA, HFSS and Analyst

GdfidL short ω/2π	GdfidL R/Q short	GdfidL long ω/2π	GdfidL long R/Q	MAFIA short ω/2π	MAFIA R/Qs	HFSS short ω/2π	Analyst short ω/2π	Analyst short R/Q	Analyst long ω/2π	Analyst long R/Q
2.44882	13.393	2.44875	14.986	2.45610	0.154	2.45421	2.44978	0.078	2.44940	14.922
2.45507	12.229	2.45475	11.471	2.46210	1.370	2.46033	2.45609	1.324	2.45344	9.948
2.46556	0.020	2.46462	0.083	2.47221	0.271	2.47039	2.46671	0.184	2.45640	0.164
2.48040	1.129	2.47772	1.308	2.48654	0.297	2.48493	2.48176	0.327	2.45985	1.202
2.49958	0.188	2.49125	0.264	2.50509	0.351	2.50383	2.50135	0.273	2.46859	0.050
2.52290	0.443	2.50140	0.024	2.52765	0.001	2.52670	2.52542	0.014	2.48288	1.122
2.54957	0.265	2.51266	0.000	2.55351	0.170	2.55297	2.55350	0.197	2.50180	0.164
2.57804	0.016	2.53200	0.215	2.58107	0.126	2.58094	2.58363	0.168	2.52473	0.312
2.61523	0.222	2.55826	0.166	2.61877	0.020	2.61766	2.64203		2.54992	0.300
2.62637	0.096	2.58672	0.012	2.62793	0.002		2.66659		2.57189	0.000

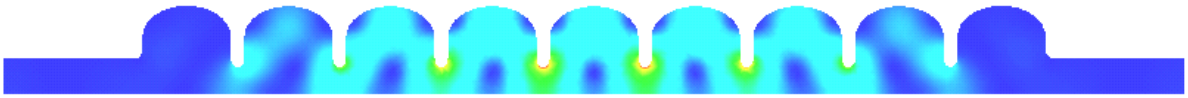

Figure 5: Analyst field plot of |E| for 1st Mode in 3rd Dipole band at a frequency of 2.4498 GHz.

Figure 6: Analyst field plot of |E| for multi-cavity mode in the 3rd dipole region at a frequency of 2 .64203 GHz

Analyst had a different beam tube lengths compared to those of the other codes used then we would not expect them all to converge to the same modes. To summarise, in the GdfidL simulations beam pipe length were chosen to be 172 mm (1.5 cell lengths) whilst in Analyst the pipes were 150 mm. We made additional simulations on the sensitivity to beam tube length. These additional simulations used beam tube lengths of 3 cells for both GdfidL and HFSS and 4.5 cells for Analyst. As expected, the modes whose field is well contained in the cavity revealed little influence on the beam tube length. For example, in the GdfidL simulations the first mode in the third band at 2.44882 GHz shifted by approximately 70 KHz (the expected accuracy being not better than several hundred kHz at best). However, modes with significant field in the end-cell and pipe region were markedly affected. The 9th mode in the 3rd band shifted down by 57 MHz from 2.615 GHz. For the Analyst result with longer beam pipes the same mode shifted down by 92 MHZ from 2.642 GHz. Thus, the first mode in the third band, which has the largest transverse R/Q is sensitive to the exact configuration of the end cells. Small perturbations in the geometry of the end cells may allow the mode to be damped by couplers located in the end cells.

Finally we note that for multi-cavity modes above the cut-off frequency, radiation boundary conditions are a more appropriate means to model the boundaries.

After performing a summation over these modes [4] the wake-field experienced by the beam can be obtained and this is described in the following section.

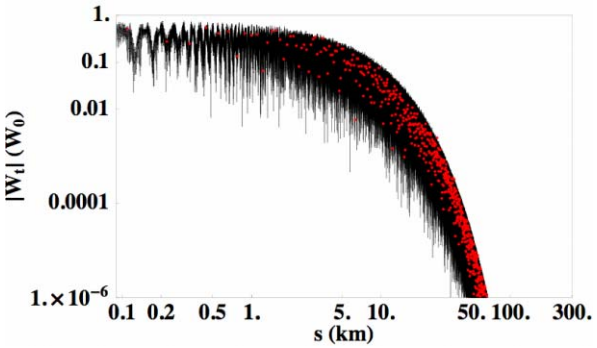

Figure 7: Envelope of the transverse component of the long-range wake-field due modes in the first three dipole bands. W_0 = 0.1472 V/pC/mm/m.

TRANSVERSE WAKE-FIELDS

In order to consider the worst-case wake-field we analysed the envelope of the wake-field rather than the field the beam experiences itself directly. Furthermore, in calculating the wake-field we limited the summation of modes [4] to that of the first 3 bands. The reason that only three bands provides an adequate description of the wake-field is that the largest R/Qs are located in these dipole bands. The wake-field trailing the first bunch in the train is illustrated in Fig.7 for a damping Q factor of

10^5. After 10 km, or approximately 100 bunches, the damping has significantly attenuated the wake-field and we note that in future beam dynamics simulations of the order of 100 bunches should be sufficient to adequately analyse the interaction mechanism.

To assess the sensitivity of the modes in diluting the emittance of the beam and causing beam instabilities we studied S_{RMS}, the RMS of the sum wake-field [7]. From past experience of making such an analysis in X-band accelerating structures values of S_{RMS} larger than unity give rise to a significant emittance dilution and in some case, beam break up. Thus, S_{RMS} is evaluated as a function of small deviation in the bunch spacing. We also note that a small fractional change in the bunch spacing corresponds to a change in the mode frequencies and will arise as a natural consequence of fabrication tolerances. The curves in Fig. 8 reveal several resonances in the vicinity of the nominal bunch spacing of 369 ns. These large peak values have the potential to give rise to significant emittance growth. Care should be taken to ensure these regions are excluded or larger damping values utilized.

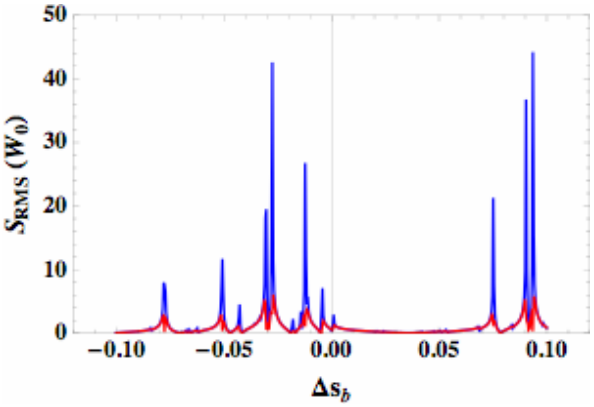

Figure 8: RMS of the sum wake-field as a function of percentage deviations in the bunch spacing. For $Q=10^6$ (blue) and $Q=10^5$ (red).

CONCLUSION

We have investigated the constituents of the long-range modes of the transverse wake-field in the latest Ichiro cavity design. A detailed comparison of current computer codes used for this purpose was undertaken. The first two dipole bands agree well to the within the numerical accuracy expected of the codes. Higher bands show significant deviations but are explained by the presence of multi-cavity modes. To properly account for these discrepancies will require complete amalgams of cavities to be modelled, or radiation boundary conditions applied. Simulations of multiple cavities are currently under investigation with a globalised scattering method [6].

The mode with the largest transverse R/Q factor is trapped within the inner cells of the cavity and in the context of the ILC, unless means are taken to perturb the geometry of the end cells, it may give rise to an appreciable amount of emittance dilution. We note a similar trapped mode was discovered in the TESLA cavities [8] and it was redistributed by perturbing the end cells in a subsequent redesign.

The RMS of the sum wake-field shows a significant sensitivity to small changes in the bunch spacing. Resonances in the vicinity of the nominal bunch spacing may indicate the presence of regions of large emmitance dilution.

ACKNOWLEDGEMENTS

We are pleased to acknowledge the assistance provided by Dr. J. DeFord and Dr. B. Held from STAAR Inc. in rapid preparation of the Analyst results. Also, we acknowledge the timely advice and support of Dr. W. Bruns, the author of GdfidL. We value the rapid communication involving data exchange on the new Ichiro cavities and useful discussions with Dr. Y. Morozumi and the encouragement in this work by Professor K. Saito.

REFERENCES

[1] N. Phinney, ICFA beam dynamics newsletter No 42, April 2007; ILCSC Parameters Document, http://www.fnal.gov/directorate/icfa/LC_parameters.pdf
[2] ILC Reference Design Report; http://lcdev.kek.jp/RDR/
[3] R. L. Geng; Review of New Shapes for Higher Gradients; Physica C, Volume 441, Issue 1-2, p. 145-150, 2006
[4] R.M Jones and C.J. Glasman; Proc. LINAC06, 2006
[5] L. Xiao *et al*; Proc. PAC07, 2007
[6] I. Shinton and R.M. Jones, this conf., SRF2007.
[7] R.M. Jones *et al.,* SLAC-PUB-8108, 1999.
[8] R. Wanzenberg, TESLA-Report 2001-33